JOURNAL OF THE KOREAN ASTRONOMICAL SOCIETY
29: 207~215, 1996

CORONAL TEMPERATURE, DENSITY AND NONTHERMAL VELOCITY DERIVED FROM SERTS EUV SPECTRA

MOON, YONG-JAE[1,2], YUN, HONG SIK[2], DAVILA, J. M.[3], AND PARK, YOUNG DEUK[1]
[1]Korea Astronomy Observatory, Taejon, 305-348
[2]Department of Astronomy, Seoul National University, Seoul 151-742
[3] Solar Physics Branch, Laboratory for Astronomy and Solar Physics,
NASA/Goddard Space Flight Center, Greenbelt, MD20771, U.S.A.
(Received September 9, 1996; Accepted October 11, 1996)

ABSTRACT

To derive coronal temperature, electron density and nonthermal velocity, we have analyzed high resolution spectra (e.g., Fe XII 338.3, Fe XII 352.1, Fe XIV 334.2, Fe XIV 353.8, Fe XV 284.2, Fe XV 321.8, Fe XV 327.0, Fe XVI 335.4, and Fe XVI 360.8) taken from AR 6615 by SERTS (Solar Extreme Ultraviolet Rocket Telescope and Spectrograph). Important findings emerging from the present study are as follows: (1) Temperature estimated from Fe XVI 335.4 and Fe XIV 334.2 is $\sim 2.4 \times 10^6$ K and no systematic difference in temperature is found between the active region and its adjacent quiet region; (2) Mean electron density estimated from Fe XV is $\sim 3 \times 10^9$ cm^{-3} and $\sim 10^{10}$ cm^{-3} from Fe XII and Fe XIV; (3) Mean density of the active region is found to be higher than that of the quiet region by a factor of 2; (4) Nonthermal velocity estimated from Fe XV and Fe XVI is $20 \sim 25$ km s^{-1} which decreases with increasing ionization temperatures. This supports the notion that the nonthermal velocity declines outwards above the transition region.

Key Words: Solar corona, EUV spectra, Non-thermal

I. INTRODUCTION

It is well known that solar EUV spectroscopy is an important tool of studying thermal structure and dynamics in the transition region and the corona. In the past, most EUV solar spectra have been obtained through several Rocket borne telescopes and spacecrafts(e.g., NRL Skylab S082A) and now SUMER and CDS instruments of SOHO are the major supplier. The solar EUV spectroscopy made on earlier observations are reviewed very nicely by Mason & Monsignori Fossi (1994) and Dwivedi (1994).

SERTS (Solar Extreme Ultraviolet Roket Telescope and Spectroscopy) developed by GSFC (Goddard Space Flight Center) is designed to study the solar corona and the transition region. The spectrograph in SERTS has a spatial resolution of about 7″ with a spectral resolution of about $60m\AA$, covering a spectral range of $175 \sim 450$ $\AA$. By comparison, the NRL skylab S082A spectrograph has a spatial resolution of 2″ with a spectral resolution of $100m\AA$, covering a spectral range of 171 to 630 $\AA$ (Dere 1978). So far a total of four observing flights (1989, 1991, 1993, 1995) has been made with the SERTS instrument on board. The first flight was made on May 5 of 1989, which resulted in a most comprehensive EUV spectral catalogue, where a total of 269 emission lines has been identified with measurements of line intensity and FWHM (Thomas & Neupert 1994). These data have been employed by Bhatia *et al.* (1994), Keenan *et al.* (1993), and Keenan *et al.* (1995) for coronal density diagnostics. The second flight data (May 7, 1991) has been used for studies of coronal temperature (Brosius *et al.* 1994).

Our main interest in this work is to examine how nonthermal velocity behaves near 2.0×10^6 K. It is well known that the nonthermal broadening varies with temperature. Mariska (1992) made an interesting study on the behavior of the nonthermal velocity in the transition region, where he noted that the nonthermal velocity increases with temperature. However, it remains uncertain whether such a tend continues increasing outward, moving into the

corona (Mariska 1992, Dere& Mason 1993, Cook *et al.* 1994). To resolve this problem, high spatial and spectral resolution spectroscopic EUV observations are needed, for sub-arcsec velocity features are detected in the transition region (e.g., Dere *et al.* 1987, Kjeldseth-Moe *et al.* 1993).

In this paper we make use of the second flight SERTS data to examine the behavior of the nonthermal velocity in the corona. For this purpose, we have selected numerous prominent Fe XII 338.3, Fe XII 352.1, Fe XII 364.5, Fe XIV 334.2, Fe XIV 353.8, Fe XV 284.2, Fe XV 321.8, Fe XV 327.0, Fe XVI 335.4 and Fe XVI 360.8 lines taken from AR6615 and its surrounding quiet region. In §II we describe briefly EUV line observations made by SERTS. In §III the detailed analysis and important findings are presented. Finally, a brief summary and conclusion will be given in §IV.

II. INSTRUMENTS AND OBSERVATIONS

SERTS is designed to make high resolution imaging spectroscopy in EUV (Neupert 1992, Brosius *et al.* 1994, Falconer 1994). As seen from Figure 1 of Brosius *et al.* (1994), it uses a 4.9′ long narrow slit and two rectangular window for imaging, which enables to perform high resolution imaging spectroscopy. The slit spectrograph mounted on SERTS 91 covers spatially 7″ with 72 pixels and spectrally 225 $\AA$ to 450 $\AA$ with 20,000 digitized pixels, thus providing a sampling size of 11 $m\AA$. SERTS 91 uses a multilayer coated diffraction grating (Davila *et al.* 1992), which is a big improvement in grating efficiency by a factor of 9 over the SERTS 89's grating. Images were recorded on Eastman Kodak 101-07 EUV sensitive photographic film and digitized with a Perkin-Elmer microdensitometer. The photometric calibrations were carried out at GSFC and at the Synchrotron Ultraviolet Radiation Facility of the National Institute of Standards and Technology. The relation between film density and log E was derived by taking the ratio of several pairs of images with different exposure. In the second flight, ten sets of data were taken, varying the exposure time ranging from 0.8 sec to 202.3 sec. The present work uses a set of spectra taken with an exposure of 202.3 sec except for Fe XVI 360.8 $\AA$, since most of the observed Fe XVI 360.8 lines were saturated. In the latter case we have used spectra exposed with 40.3 sec. The atmospheric extinction, film sensitivity, and the overall instrumental sensitivity have been corrected in accordance with Davila (1995).

III. ANALYSIS AND RESULTS

(a) Line Fitting

We have analyzed spectra taken from active region AR6615 and its surrounding region. Since He II 303 $\AA$ line is the most prominent line within the spectral range under consideration, our wavelength calibration has been referenced to the line. The wavelength calibration has been made, using the following conversion equation

$$\lambda(A) = 303.78222 + 0.010979C - 4.021943 \times 10^{-10}C^2 - 5.62688 \times 10^{-15}C^3, \quad (1)$$

where C is a pixel position relative to the He II 303 centroid. The rest of the observed lines are identified with equation (1) together with the EUV catalogue of Thomas & Neupert (1994), and their FWHM is estimated by fitting line profiles with a Gaussian and quadratic polynomial

$$I(x) = A_0 \exp(-(x - A_1)^2/A_2) + A_3 + A_4x + A_5x^2, \quad (2)$$

where A_i are fitting parameters and x is a wavelength.

(b) Temperature Diagnostics

Under the coronal condition of low density and high temperature the collisional excitation is dominant over ionization and recombination and the radiative deexcitation is the main means of depopulation. Accordingly, the rate of emission per unit volume for a spectral line can be approximated as

$$P_{jk} = N_i N_e C_{gj} B_{jk} E_{jk}, \quad (3)$$

where g refers to the ground state, j to the upper state and k, to the lower state. Here N_i is the number density of an ion, N_e is the number density of electrons, B_{jk} is the branching ratio or radiative decay coefficient, and E_{jk} is the energy of the emitted photon. And C_{gj}, the collisional excitation coefficient given by

$$C_{gj} = 8.63 \times 10^{-6}(\omega_{gj}/w_g T^{1/2}) \exp(-E_{gj}/kT), \tag{4}$$

where w_g is the statistical weight of the ground state, k is the Boltzmann constant, E_{gj} is the energy from the ground state to the excited state, ω_{gj} is the thermally-averaged collision strength. Then the intensity ratio of two lines associated with different stage of ionization can be expressed as

$$\frac{I_a}{I_b} = \frac{(N_i/N_E)_a E^a_{jk} B^a_{jk} \omega^a_{gj} w^b_g}{(N_i/N_E)_b E^b_{jk} B^b_{jk} \omega^b_{gj} w^a_g} \exp[(E^b_{gj} - E^a_{gj})/kT], \tag{5}$$

where N_i/N_E is the fraction of ionization in the ith stage of a given element.

Brosius (1995) derived equation (6) to relate temperature to line ratio for numerous EUV lines applicable for densities ranging from $N_e = 10^9/cm^3$ to $N_e = 10^{10}/cm^3$, which is given by

$$\log T = a0 + a1 \log R + a2(\log R)^2 + a3(\log R)^3 \tag{6}$$

where R is the intensity ratio of two selected lines. In this case, the fitting parameters are $a0 = 6.236$, $a1 = 0.109$, $a2 = 7.83 \times 10^{-3}$, $a3 = 1.97 \times 10^{-3}$ for $n_e = 10^9 cm^{-3}$, and $a0 = 6.218$, $a1 = 0.107$, $a2 = 6.67 \times 10^{-3}$, $a3 = 2.07 \times 10^{-3}$ for $n_e = 10^{10} cm^{-3}$, respectively.

The intensity ratio of various observed lines has been measured. It is found that a pair of Fe XVI 335.4 and Fe XIV 334.2 lines yield best fit to the Brosius formula (Brosius 1995). Accordingly, a total of 53 pairs of Fe XVI 335.4 and Fe XIV 334.2 line profiles has been taken to measure their integrated intensity and FWHM. The measured intensity is plotted as a function of position in Figure 1, where the standard deviation is calculated by the method described in Thomas & Neupert (1994). The electron temperature is estimated by substituting the measured intensity ratio, I(Fe XVI 335.4)/I(Fe XIV 334.2) into equation (6). The temperature estimated at various locations along the slit is presented in Figure 2. The "active region" in the figure refers to a region in which Fe XVI 335.4 line intensity exceeds 4,000 $erg/cm^2/sec$. The mean temperature averaged over the entire region along the slit region is about log T = 6.36 for $N_e = 10^{10} cm^{-3}$ and log T = 6.38 for $N_e = 10^9 cm^{-3}$. These estimates are a little larger than their respective ionization equilibrium temperatures (Arnaud & Raymond 1992). No systematic difference is noted in temperature between the active region and its surrounding quiet region (see Fig. 2).

(c) Density Diagnostics

Density diagnostics are made by taking line intensity ratio for a pair of lines of the same ion. In our density diagnostics we have selected seven iron coronal lines (see Table 1) originated from three different stages of ionization (Fe XII, Fe XIV and Fe XV). First we fit the observed profiles, using equation (2). The resulting parameters which fit best to these profiles are listed in Table 1, where they are compared with those obtained from SERTS 89 (Thomas & Neupert 1994). The integrated intensities derived from SERTS 91 are very similar to those from SERTS 89 except for very weak Fe XV 321.8 line. The accuracy of 91 data is far better than that of 89 data, which seems to be attributed to the improvement made in the grating efficiency for SERTS 91. The electron number density is derived from intensity ratio of Fe XII and Fe XIV with the use of the theoretical result of Brickhouse et al. (1995) (see Fig. 3 and Fig. 4). The electron number density derived from Fe XII lines (I_{12} and I_{13} in Table 2) is a little larger than that obtained from Tayal *et al.* (1989). In the case of Fe XIV (I_{45} in Table 2), our estimate is larger than that obtained from Bhatia *et al.* (1994) by a factor of 2. These estimates are summarized in Table 2 and are compared with those estimated from SERTS 89 data. According to our analysis the electron density in the active region B (35-49 in pixel position) is found to be 1.3×10^{10} $/cm^3$, which is higher than that of the quiet region by a factor of 2. The electron density estimated from Fe XV 321.8 and Fe XV 327.0 with the use of the theoretical result (Fig. 2 of Dufton *et al.* 1990) is found to be $3 \times 10^9 cm^3$.

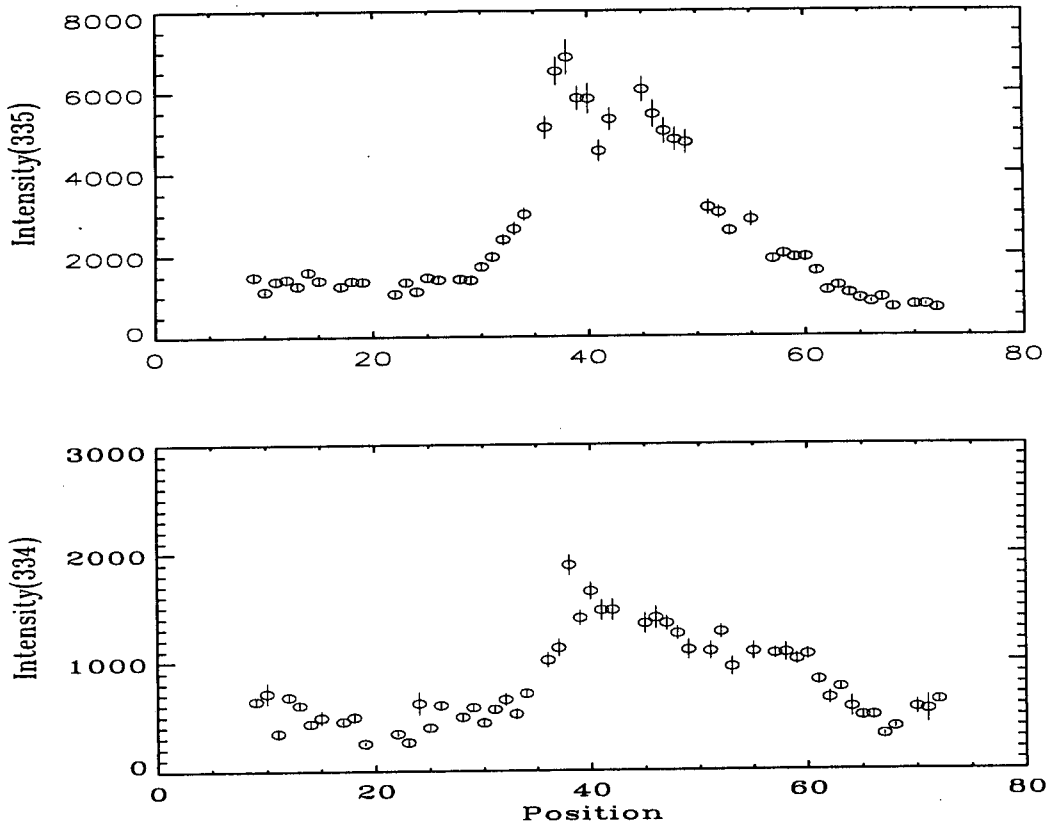

Fig. 1. Measured total intensities of Fe XVI 335.4 and Fe XIV 334.2, where they are plotted as a function of position along the slit.

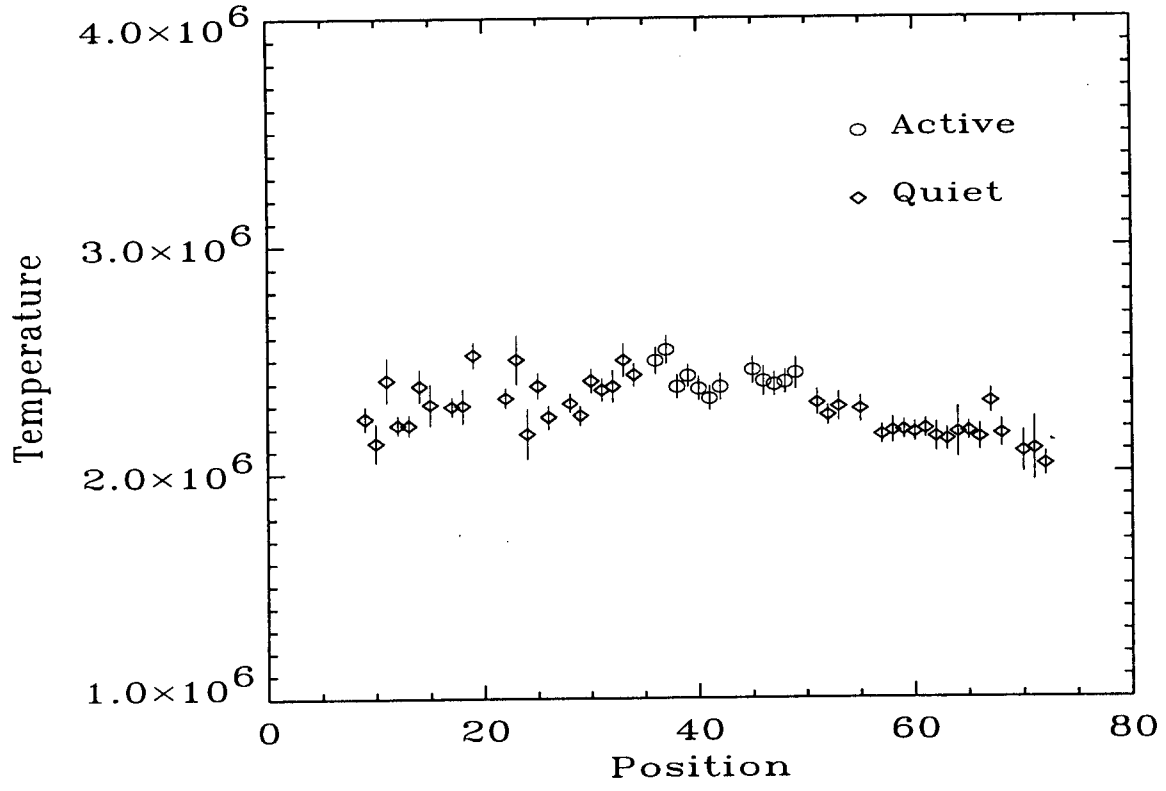

Fig. 2. Temperature estimated from measured intensity ratio, I(Fe XVI 335.4)/I(Fe XIV 334.2), where it is plotted as a function of position along the slit.

Table 1. Fitting results of seven EUV lines from SERTS 91 data

ID	Element	λ_0^a	λ^b	I	σ_I	I^c	σ_I^c
1	Fe XII	338.26	338.29	75.5	3.6	76.6	10.3
2	Fe XII	352.10	352.12	249.6	12.5	249.0	26.0
3	Fe XII	364.47	364.48	178.9	11.0	144.0	17.0
4	Fe XIV	334.17	334.19	742.4	37.4	642.0	73.0
5	Fe XIV	353.83	353.85	374.1	19.8	291.1	33.0
6	Fe XV	321.79	321.77	12.3	0.6	35.4	7.9
7	Fe XV	327.02	327.05	82.2	4.1	87.5	12.5

[a] Referenced wavelength from Brickhouse et al. (1995) for Fe XII and Fe XIV and from Dufton et al. (1990) for Fe XV.

[b] Estimated wavelength from SERTS 91 data

[c] From SERTS 89 data (Thomas & Neupert 1994)

Table 2. Intensity ratio and electron number densities derived from SERTS 91 data

R(Intensity ratio)	Element	log T	log R	log N_e	log R[a]	log N_e^a
I_{12}	Fe XII	6.1	-0.37 ± 0.03	9.9	-0.27 ± 0.07	10.1
I_{13}	Fe XII	6.1	-0.52 ± 0.03	9.9	-0.51 ± 0.08	9.9
I_{45}	Fe XIV	6.3	0.3 ± 0.03	10.0	0.3 ± 0.07	10.0
I_{76}	Fe XV	6.3	0.82 ± 0.03	9.2	0.39 ± 0.12	9.7

[a] From SERTS 89 data (Thomas & Neupert 1994)

(d) Nonthermal Velocity Diagnostic

Since our observed line profiles are Gaussian, the nonthermal velocity can be estimated from

$$W^2 = W_{th}^2 + W_{nt}^2 + W_{inst}^2. \tag{7}$$

by measuring the full width at half-maximum of each line. The instrumental width, W_{inst} is estimated from the laboratory. The estimated instrumental broadening for SERTS 91 is presented in Figure 5. Once the instrumental broadening is removed, the line width is given by

$$W_D = \sqrt{W_{th}^2 + W_{nt}^2} = \frac{\lambda_0}{c}(2kT/M + \xi^2)^{1/2}, \tag{4}$$

where M is the mass of the atom and ξ is the nonthermal velocity. Therefore, the nonthermal width can be easily calculated, once the temperature is known. The temperature can be estimated either by measuring line intensity ratio of a pair of temperature sensitive lines or by simply taking ionization equilibrium temperature of the ion under consideration.

In the present work the nonthermal velocity is estimated, making use of the ionization equilibrium temperatures 2.0 $\times 10^5$ K for Fe XV 284.2 and 2.2 $\times 10^5$ K for Fe XVI 335.4 and Fe XVI 360.8, respectively (Arnaud & Rothenflug 1985). The resulting estimates are plotted in Figure 6 through Figure 8 as a function of position along the slit. In the figures the data points having negative W_{nt} have been neglected. As can be seen from these figures, the estimated nonthermal velocity ranges from 19.5 km/s to 24.9 km/s with no systematic difference between the active and its surrounding quiet region and it decreases with increasing temperature, which supports the notion that the nonthermal velocity could decline outwards above the transition region.

IV. A SUMMARY AND CONCLUSION

In this paper we made use of SERTS 91 data to examine the behavior of the nonthermal velocity in the corona. For this purpose, we have selected numerous prominent Fe XII 338.3, Fe V 284.2, Fe XIV 334.2, Fe XVI 335.4 and

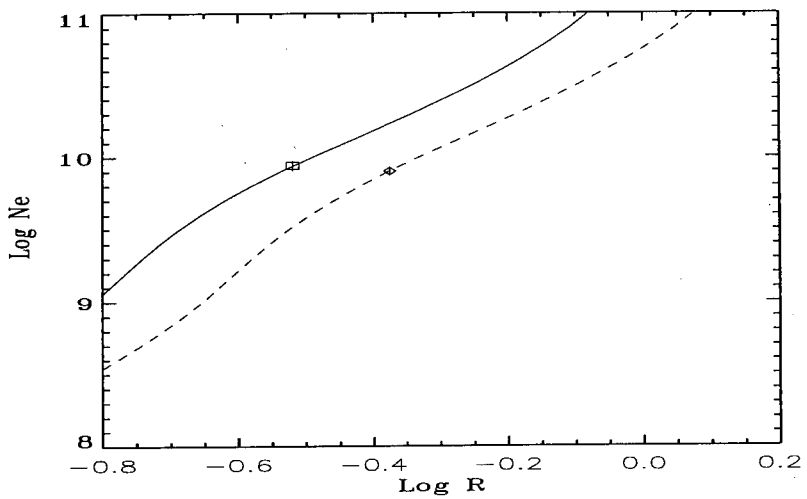

Fig. 3. Brickhouse et al.'s theoretical relation between intensity ratio of a pair of Fe XII lines and electron number density(Brickhouse et al. 1995). The solid line refers to I_{12}=I(Fe XII 338.3)/I(Fe XII 352.1) and the dotted line, to I_{13}=I(Fe XII 338.3)/I(Fe XII 364.5).

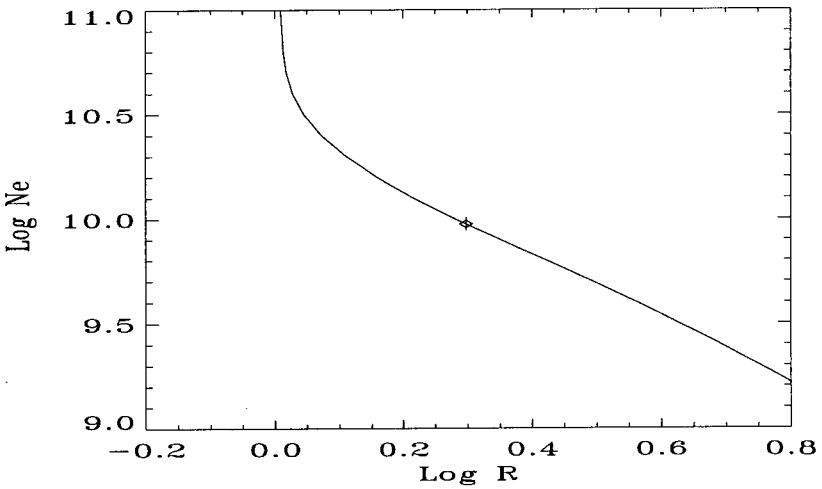

Fig. 4. Brickhouse et al.'s theoretical relation between intensity ratio of a pair of Fe XIV lines and electron number density(Brickhouse et al. 1995). The solid line refers to I_{45}=I(Fe XIV 334.2)/I(Fe XIV 353.8).

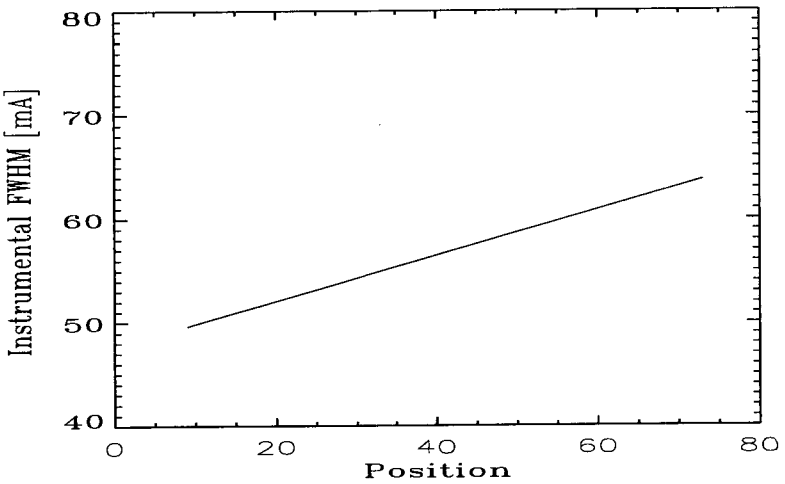

Fig. 5. Instrumental FWHM of SERTS 91 plotted as a function of pixel position.

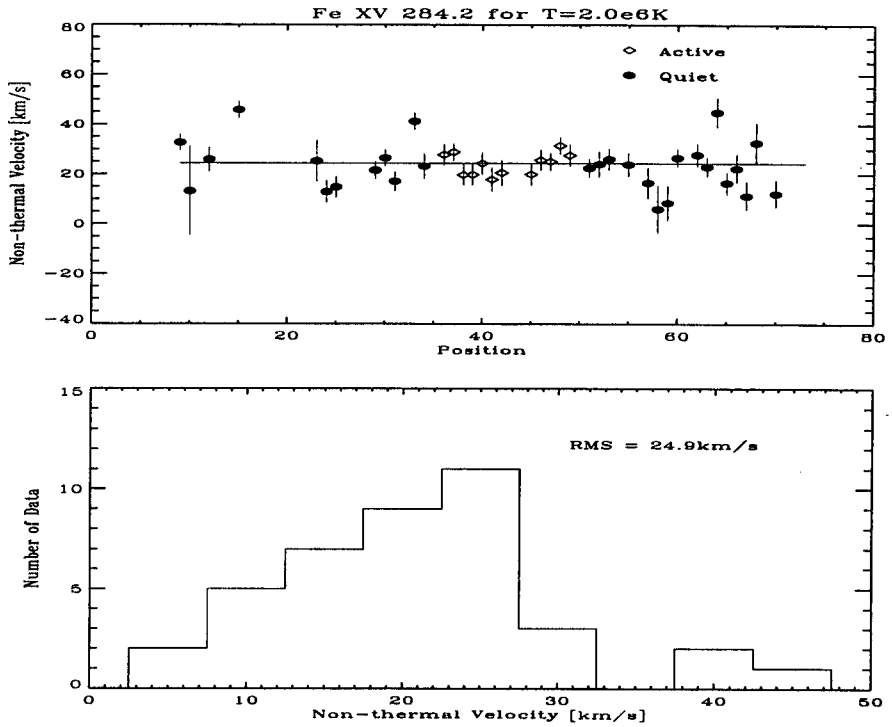

Fig. 6. Nonthermal velocity estimated from Fe XV 284.2, where they are plotted as a function of position along the slit. Histogram yields a nonthermal velocity of 24.9 km/s. The straight line refers to the thermal velocity estimated with the use of Fe XV's ionization equilibrium temperature of 2.0×10^6K.

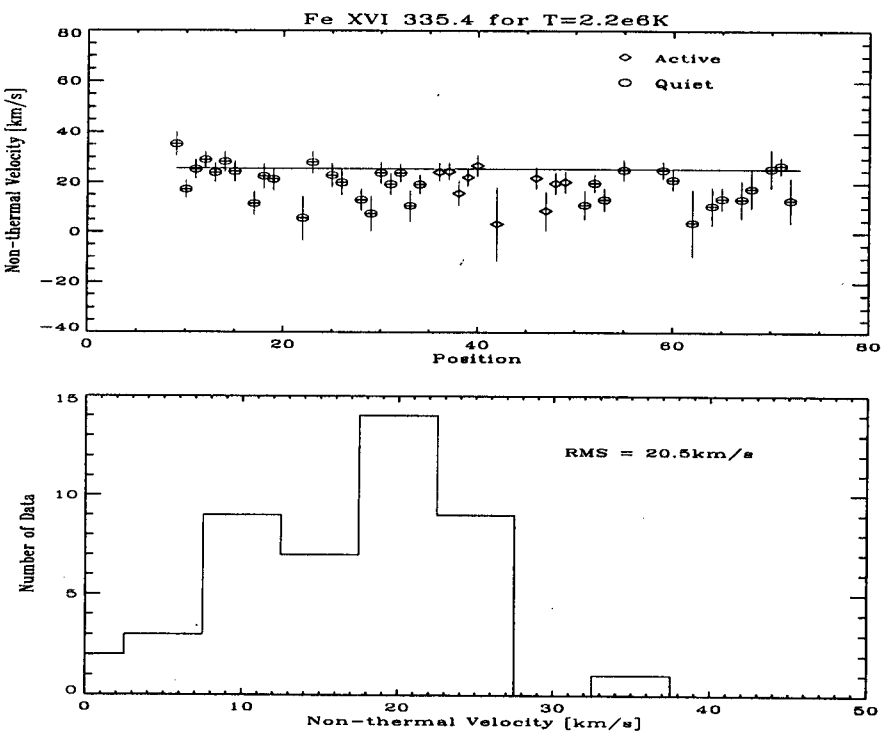

Fig. 7. Nonthermal velocity estimated from Fe XVI 335.4, where they are plotted as a function of position. Histogram yields a nonthermal velocity of 20.5 km/s. The straight line refers to the thermal velocity estimated with the use of Fe XV's ionization equilibrium temperature of 2.2×10^6K.

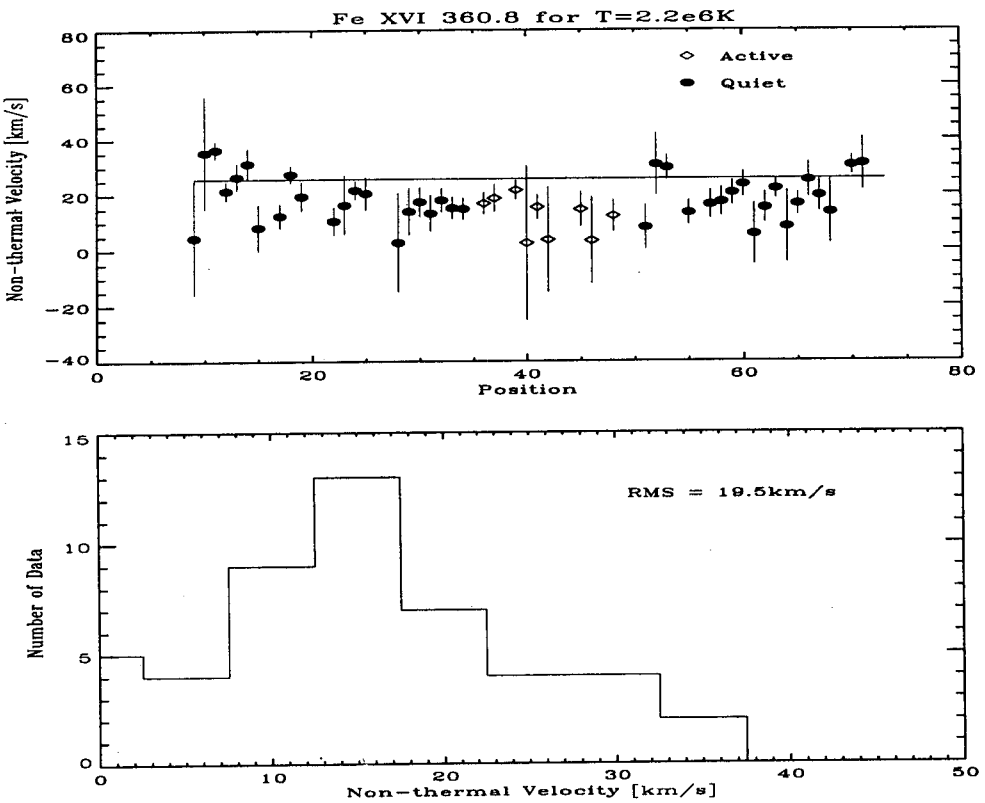

Fig. 8. Nonthermal velocity estimated from Fe XVI 360.8, where they are plotted as a function of position. Histogram yields a nonthermal velocity of 19.5 km/s. The straight line refers to the thermal velocity estimated with the use of Fe XV ionization equilibrium temperature of 2.2×10^6K.

Fe XVI 360.8 lines taken from AR6615 and its surrounding quiet region. From these spectra temperature, electron density and nonthermal velocity were derived. In analyzing these data He II 303 line was used as a reference for wavelength calibration and the observed lines were identified with the use of equation (1) together with the EUV catalogue of Thomas & Neupert (1994). The total intensity and FWHM have been measured by fitting line profiles with a gaussian and quadratic polynomial. For temperature determination we made use of Brosius's empirical relation and for density diagnostics line ratio technique was applied to iron lines originated from three different stages of ionization, Fe XII, Fe XIV and Fe XV. With the temperature estimated from the present analysis the nonthermal velocity has been estimated.

Some of the important findings emerged from the present work are as follows: (1) the coronal temperature determined from the intensity ratio of Fe XVI 335.4 to Fe XIV 334.2 is about $\sim 2.4 \times 10^6$ K and no systematic difference is found between the active and its adjacent quiet region. (2) the mean electron density estimated from Fe XII and Fe XIV lines is about 10^{10} cm^{-3} and is about 3×10^9 cm^{-3} from Fe XV lines (see Table 2) and the mean density of the active region is found to be higher than that of the quiet region by a factor of 2. (3) The nonthermal velocity obtained from prominent Fe XV 284.2, Fe XVI 335.4, and Fe XVI 360.8 lines is found to be about 20 km/s and it decreases with increasing ionization equilibrium temperature, supporting the notion that the nonthermal velocity declines outwards above the transition region.

ACKNOWLEDGEMENT

We (YJM, HSY, and YDP) would like to express our sincere gratitude to Dr. A. I. Poland for his hospitality during a month visit to Goddard, NASA in July, 1995 and to Dr. R. J. Thomas and Dr. J. W. Brosius for helpful discussions. This work is supported by The Basic Science Research Institute Program, Ministry of Education, ROK, 1995 (BSRI-95-5408). YJM and YDP are very thankful for research fund from Korea Astronomy Observatory.

REFERENCES

Arnaud, M. & Raymond, J. 1992, ApJ, 398, 394
Arnaud, M. & Rothenflug, R. 1985, A&AS, 60, 425
Bhatia, A. K., Kastner, O. S., Keenan, F. P., Colon, E.S., & Widing K.G. 1994, ApJ, 427, 497
Brickhouse, N. S., & Raymond, J. C., & Smith B. W. 1995, ApJS, 97, 551
Brosius, J. W., Davila, J. M., Thomas, R.J., & Thompson, W. T. et al. 1994, ApJ, 425, 343
Brosius, J. W. 1995, private communication
Cook, J. W., Keenan, F. P., Harra, L. K., & Tayal, S. S. 1994, ApJ, 429, 924
Davila, J. M., Thomas, R. J., Thompson, W. T., et al. 1992, in Proc. 10th Int. Conf. on UV and Spectroscopy of Astrophysical and Laboratory Plasmas
Davila, J. M. 1995, private communication
Dere, K. P. 1978, ApJ, 221, 1062
Dere, K. P., Bartoe, J.-D. F., Bruckner, G. E., Cook, J. W., & Socker, D. G. 1987, Solar Phys., 114, 223
Dere, K. P. & Mason, H. E. 1993, Solar Phys., 144, 217
Dufton, P. L., Kingston, A. E., & Widing, K. G. 1990, ApJ, 353, 323
Dwivedi, B. N. 1994, Space Science Rev., 65, 289
Falconer, D. A. 1994, NASA Technical Memorandum 104616.
Keenan, F. P., Thomas, R. J., Neupert, W. M., Colon, E. S., & Burke, V. M. 1993, Solar Phys., 144,69
Keenan, F. P., Greer, C. J., Foster, V. J., & Widing K. G., 1995, Solar Phys., 161, 159
Kjeldseth-Moe, O., Brynildsen, N., Brekke, P., Maltby, P., & Brueckner, G. E. 1993, Solar Phys., 145, 257
Mariska, J. T. 1992, in The Solar Transition Region, p. 117
Mason, H. E., & Monsignori Fossi, B. C. 1994, A&A Rev., 6, 123
Neupert, W. M., Epstein, G. L., Thomas, R. J., & Thompson, W. T. 1992, Solar Phys., 137, 87
Tayal, S. S., Henry, J. W., Keenan, F. P., McCann, S. M., & Widing, K. G. 1989, ApJ, 343, 1004
Thomas, R. J. & Neupert, W. M. 1994, ApJS, 91, 1